Paper

Modeling the Luminance Distribution of 3-D Object Surface with Specular Reflection Component and Shape Measurement

Naotaka IKEMOTO, Kenji FUJINAMI*, and Minoru ISOMURA
Nihon University
*Koito Industries, LTD

Paper originally published in Japanese in J.IEIJ, Vol.84, No.8A, 2000

ABSTRACT

A method is described for reducing the large error that often occurs in the measurement of three-dimensional (3D) objects using the photometric stereo method when there is a specular component in the reflection characteristics of the object's surface. First, the change in the luminance distribution caused by the component is estimated based on the correlation between the modeled distribution and a gray-level image of the object, created by numerical experiment. Next, the shape measurement of the hemisphere object was carried out. Numerical experiment of three dimensional measurement of a hemispherical object showed that the mean error of normal vector can be reduced by as much as 90%. This method is applicable to machine vision, automatic manufacturing, and other industrial processes.

KEYWORDS: luminance distribution model, specular refrection component, 3-D shape measurement, gray-level image

1. Introduction

Studies on extracting three-dimensional information from images input from camera[1)-3)] are important and indispensable for industrial robot object recognition.

Generally, two methods can be considered for extracting information from image data. One is a method that uses special light sources and slit light in order to calculate the absolute distance to the object from the camera. The other is the photometric stereo method[4)-8)] by which three-dimensional information from multiple gray-level images is extracted.

The photometric stereo method, a representative method for three-dimensional image measurement, is one in which gradients of the object surface based on gray-level images obtained through a device such as CCD camera are measured. The advantages of this method are its capability of measuring gradients of the object surface at every picture element of the gray-level images photographed and of obtaining a large volume of data through one measurement. In this method, multiple gray-level images are photographed, and normally, the conventional need for complicated calculations to make adjustments between images in order to fix the relative positions of the viewpoint and the object can be eliminated, thus the process of measurement is simplified and shortened. The drawback to this method is its incapability to obtain the normal vector of the object surface when the relation between the luminance and the surface gradient is unknown due to the absence of information such as the ratio of specular reflection component in surface reflection characteristics and the reflection characteristics hemselves.

To solve this, Iwahori et al.[9)] proposed a method to estimate the reflection characteristics of the object surface based on information obtained from a unique point on the surface. However, as this method requires repetitious calculations and massive processing work, the benefit of the photometric stereo method can no longer be obtained. Ikeuchi[10)] proposed another method to calculate the gradient of the target point by selecting non-highlighted gray-level images of the object surface. However, this method has also a drawback, which is that more numbers of gray-level images must be photographed.

The purpose of this study is to measure the three-dimensional shape of an object when its surface reflection characteristics are unknown by applying the photometric stereo method. To achieve this goal, gray-level images of the object surface are created using the conventional Phong model, and effects of highlight caused by the surface specular reflection component both on the measurement of normal vector and on the three-dimensional measurement of hemispheric objects are clarified.

Moreover, a method to correct gray-level images by estimating luminance distribution of highlight generated by the specular reflection component is proposed. Through numerical experiments, the effectiveness of the proposed highlight correction method is indicated.

Excerpts from this paper was addressed by Kenji Fujinami at the National Convention of the Illuminating Engineering Institute of Japan in 1998.

2. The Principle of the Photometric Stereo Method

The brightness (luminance) of the object surface can be measured by the reflection of the light, when the surface is illuminated and observed from the viewpoint.

The luminance of the object surface is determined by such factors as, the luminous intensity of the light source, the relative positions between the light source and the viewpoint, and the reflection characteristics and gradient of the object surface.

Hence, the luminance of the object surface contains information on the surface gradient. The principle of the photometric stereo method is to measure the surface gradient by effectively utilizing this fact.

In the photometric stereo method, the gradient of the object surface is measured by observing luminance level at a uniform viewpoint according to various light source positions. During the measurement process, the luminance of the object surface can be observed by photographing gray-level images by a device such as CCD camera.

Fig. 1 shows the concept of measuring the shape of the object by using the photometric stereo method. As indicated in this figure, the object is placed on the *x-y* plane on the *x-y-z* coordinates and illuminated by the light sources. The light source is regarded as a point source, and the surface of the object is assumed to be a Lambertian surface. Then, the luminance L of an arbitrary point P on the object surface is indicated by the following equation [8].

$$L=\frac{I}{r_{\mathrm{p}}^{2}\pi}\rho\cdot\cos\theta=\frac{I}{r_{\mathrm{p}}^{2}\pi}\rho\cdot\frac{\vec{N}\bullet\vec{S}}{|\vec{N}|\cdot|\vec{S}|} \qquad (1)$$

where,

$\vec{N}$: normal vector of the object surface at the point P,

$\vec{S}$: directional vector of the straight line connecting the point P and the light source,

θ :angle between $\vec{N}$ and $\vec{S}$, r_{p} : distance from the light source to the point P,

I: luminous intensity of the light, ρ : reflectance of the surface.

The luminance of the point P observed from the viewpoint is L_i, L_j and L_k, according to the position of the light source i, j and k, respectively. Therefore, let the vectors directed from the point P to each light source be S_i, S_j and S_k, and the distance between the point P and each light source be r_{pi}, r_{pj} and r_{pk}, then. L_i, L_j and L_k are described as follows:

$$\left.\begin{aligned}L_{i}&=\frac{I}{r_{pi}^{2}\pi}\rho\cdot\frac{\vec{N}\bullet\vec{S}_{i}}{|\vec{N}|\cdot|\vec{S}_{i}|}\\L_{j}&=\frac{I}{r_{pj}^{2}\pi}\rho\cdot\frac{\vec{N}\bullet\vec{S}_{j}}{|\vec{N}|\cdot|\vec{S}_{j}|}\\L_{k}&=\frac{I}{r_{pk}^{2}\pi}\rho\cdot\frac{\vec{N}\bullet\vec{S}_{k}}{|\vec{N}|\cdot|\vec{S}_{k}|}\end{aligned}\right\} \qquad (2)$$

The normal vector $\vec{N}$ of the object surface at the point P can be derived from (2). Obtaining $\vec{N}$ for all points on the object surface, the distribution of gradients (hereinafter "normal vector distribution") can be obtained.

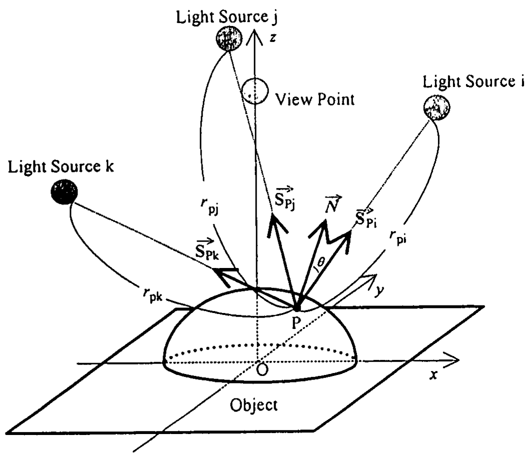

Fig. 1 The geometric relation between viewpoint, object and light source.

The luminance of the surface can be obtained even when the surface is not a Lambertian surface, since the luminance is dependent on the gradient. Therefore, the normal vector distribution of the object surface can be measured provided that the relative position of the light source, the viewpoint and the object are examined and that the characteristics of reflection of the object surface are verified.

3. Producing Gray-Level Image using the Phong Model

The luminance distribution of the object surface is calculated based on the conventional Phong model in order to produce gray-level image. The Phong model is a method to calculate the luminance of the object surface by regarding the luminance as a combination of the luminance caused by diffuse reflection and that by specular reflection.

Fig. 2 shows an example of luminous distribution of reflection of the object surface, which has a specular reflection component calculated by Phong model. The luminance L measured at the viewpoint P is given as follows.

$$L=\frac{I}{r_{\mathrm{p}}^{2}\pi}\rho_{d}\frac{\vec{N}\bullet\vec{S}}{|\vec{N}|\cdot|\vec{S}|}+\frac{I}{r_{\mathrm{p}}^{2}}\frac{|\vec{N}|\cdot|\vec{V}|}{(\vec{N}\bullet\vec{V})}\rho_{s}(\theta)(\vec{V}\bullet\vec{R})^{n} \qquad (3)$$

where,

$\vec{N}$: normal vector of the surface, $\vec{V}$: directional vector of viewing,

$\vec{S}$: directional vector of illumination, $\vec{R}$: directional vector of reflection,

r_p: distance between the light source and measuring point,

I: luminous intensity of the light source

ρ_d: diffuse reflectance, θ : angle of incidence of the light
$\rho_s(\theta)$: function of specular reflectance characteristics [12)]
n: rate of diffusion of light of specular reflection component.

In equation(3), function of specular reflectance characteristics $\rho_s(\theta)$, which indicates specular reflection against incident angle is described as follows:

$$\rho_s(\theta)=\rho_s(0)+(1-\rho_s(0))\cdot\left(\frac{2\theta}{\pi}\right)^{n_0} \qquad (4)$$

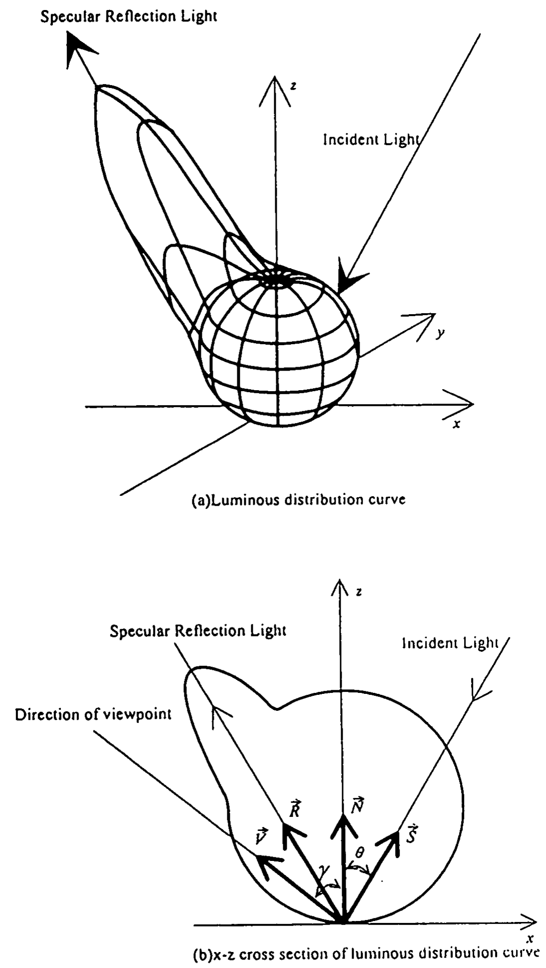

Fig.2 The luminous distribution curve of the Phong model.

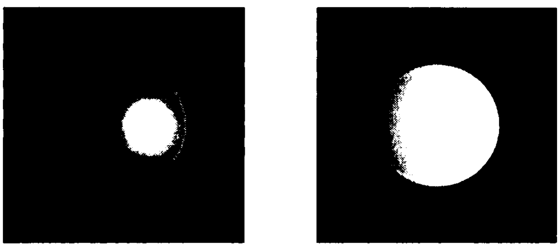

(a)Case in which the amount of specular reflection component $\rho_s(0)$ is large

(b)Case in which directivity of specular reflection light n is high

Fig.3 Comparison of gray-level images by reflection characteristics of the object surface.

where $\rho_s(0)$ is specular reflectance of the incident angle 0 [rad], and n_0 is the rate of change in luminance reflectance.

In numerical experiment, picture elements of gray-level image are 512 (horizontal) × 512 (vertical) and luminance is described based on 256 isoluminance gray-scale values (proportional to luminance L) ranging from 0 to 255. In other words, gray-level image is produced by calculating luminance of the object using equation (3) and by quantizing the image into 512 (x-axis) × 512 (y-axis) elements and expressing each element on a 256 gray scale.

Fig. 3 shows the relation between reflection characteristics and gray-scale images. Fig. 3 (a) is a gray-level image where the ratio of specular component to the total reflectance of the object surface is high, while (b) is that where the directivity of the specular reflection component is high.

4. Numerical Experiment of Three-dimensional Shape Measurement of Object

Fig. 4 is a measurement environment assumed for the numerical experiment. The object is placed on a plane (called reference plane) with 0 [%] reflectance, which is parallel to the x- and y-axes on the xyz coordinates and z = 0. The object is illuminated from the point source, of which distance from the origin O is r.

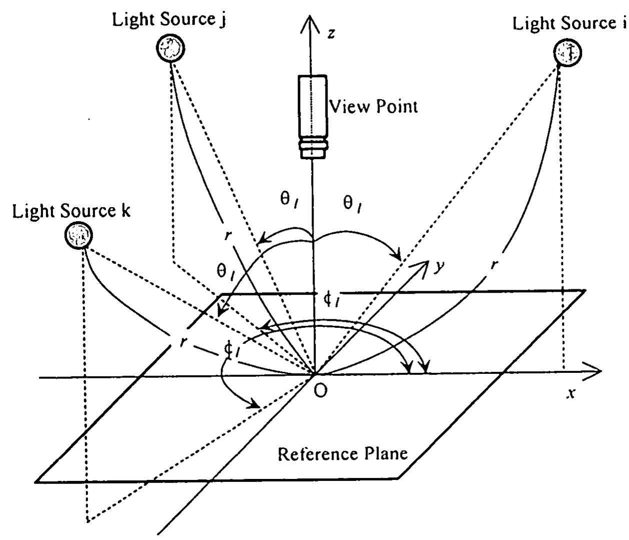

Fig.4 Measurement environment for numerical experiment.

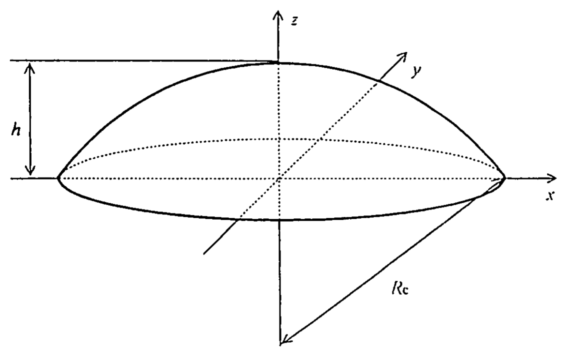

Fig.5 Shape of the object for the numerical experiment.

In order to acquire three gray-level images which are required when applying the photometric stereo method, the light sources are set in the following three positions: 1) azimuth angle ϕ_l to the x-axis =0; 2) azimuth angle ϕ_l to the x-axis =120; and 3) azimuth angle ϕ_l to the x-axis =240. For each position, the distance from the origin O is r and zenith degree is 30. The above three positions of light source are hereinafter referred to as i, j, and k, respectively. The object is photographed at the viewpoint of z =0.5r on the z-axis. As indicated in Fig. 5, the object is regarded as hemispherical with the curvature radius R_c of 0.04r and the height h of 0.01r, and with uniform reflection characteristics on the entire surface.

4.1 Effect of Specular Reflection Component of the Object Surface

In this section, the effect of specular reflection component of the object surface on measurement in the photometric stereo method is described.

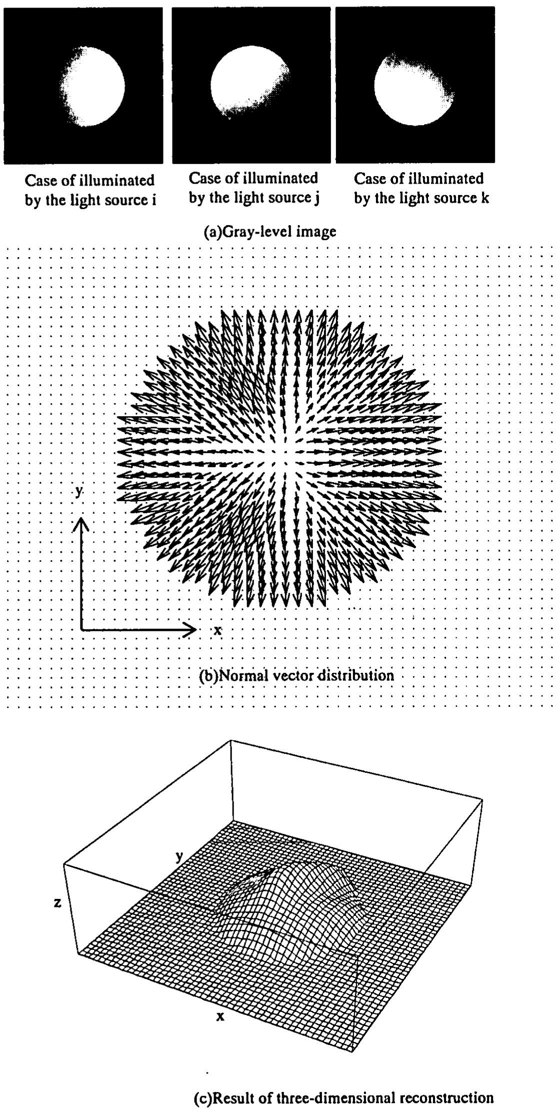

Fig.6 The numerical experiment results.

Fig. 6 is one of the measurement results of the object with a specular reflection component. Fig. 6 (a) is the three gray-level images used for measurement, (b) is the distribution of normal vector of the object surface calculated by means of the photometric stereo method, and (c) is the result of three dimensional reconstruction of the object derived from (b). Here, the diffuse reflectance ρ_d, the specular reflectance ρ_s (0) and the rate of diffusion of light of specular reflection are 0.6, 0.1, and 20, respectively.

The result shows that the shape of the three-dimensional reconstruction is different from that of the actual object, which means that correct information of the three-dimensional shape is not extracted.

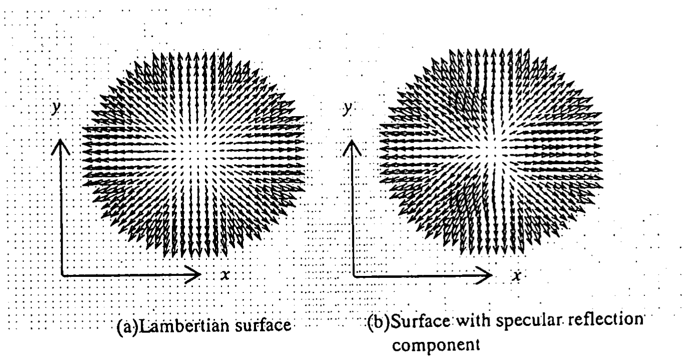

Fig.7 The comparison of normal vector distributions by reflection characteristics of the object surface.

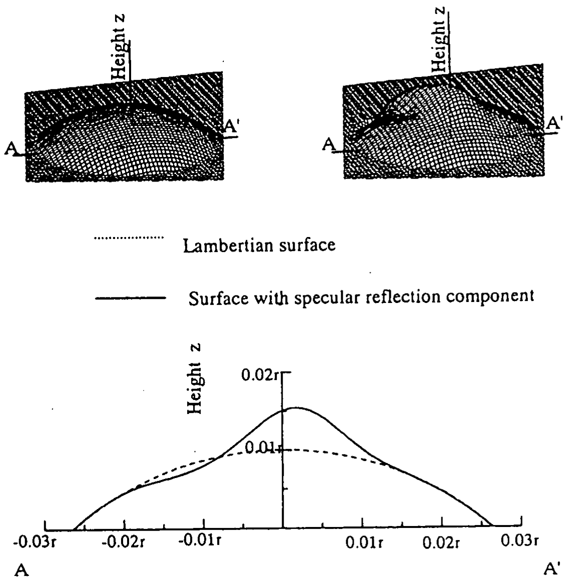

Fig.8 The comparison of two-dimensional cross section of the reconstruction results by the reflection characteristics.

Fig. 7 is a comparison of normal vector distributions for two types of object surfaces; one with a specular reflection component and the other is a Lambertian surface.

In Fig. 7 (a), the object is with Lambertian surface, while in (b), the object surface has a specular reflection component. Total reflectance of the Lambertian surface is set to 0.7, which is the same as that of the surface with a specular reflection component.

As shown in Fig. 7, normal vector distribution of the object with a specular reflection component is different from that of the Lambertian surface in the area where highlight is generated by the effect of specular reflection component. The relative height of the objects is calculated based on the above-mentioned normal vector distribution. Fig. 8 shows an example of comparison of the heights in the two-dimensional cross section between the surface with specular reflection component and the Lambertian surface. The former is indicated as a solid line, while the latter as a dotted line. As shown in Fig.8, the two-dimensional cross section of the Lambertian surface tends to be consistent with that of the actual object. On the other hand, the two-dimensional cross section of the surface with specular reflection component differs largely from that of the actual object near the zenith. As indicated in normal vector distribution, this discrepancy is due to the highlight generated by the specular reflection component.

Fig. 9 is an example of mean error of the normal vector against the specular reflectance $\rho_s(0)$ included in the total reflectance $\rho=0.7$ of the object surface. The horizontal axis of Fig. 9 represents the specular reflectance $\rho_s(0)$, while the vertical axis represents the mean error. In this graph, the symbols ○,△ and □ refer to rate of diffusion of light(n) of specular reflection component, and n is 20, 60 and 100, respectively. Here, the discrepancy of normal vector is defined as the angle between two normal vectors, namely normal vector distribution of the object with Lambartian surface and that of the object with specular reflection component, at the some position of the object.

As shown in the graph, regardless of the value of rate of diffusion of light of specular reflection component n, mean error of the normal vector increases as specular reflectance coefficient $\rho_s(0)$ rises, since highlight is enhanced.

When the coefficient n, which indicates the rate of diffusion of light of specular reflection light, is lowered, the mean error of the normal vector increases due to the reduction of directivity of the specular reflection light and thus generating highlight in a larger area According to these results, it can be concluded that the error of three-dimensional measurement of the object increases as the highlight generated by the specular reflection component on the surface is enhanced or the highlight area is widened.

4..2 Estimate of Luminance Distribution by Highlight and Its Correction

In the previous section, the errors in the shape of the object with specular reflection component when measured by the photometric stereo method are described. Errors are significant in the area that highlight is generated on the gray-level images. Therefore, shape measurement by photometric stereo method of the object with specular reflection component becomes possible if gray-level image is corrected by estimating the luminance distribution highlight generated on the object surface.

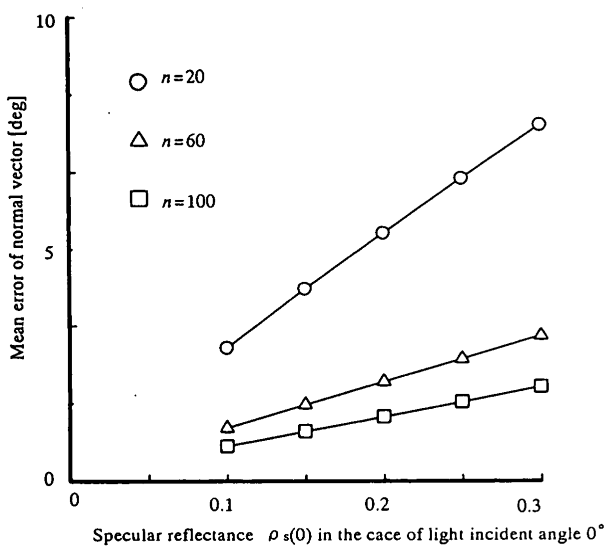

Fig.9 The mean error of normal vector for specular reflectance.

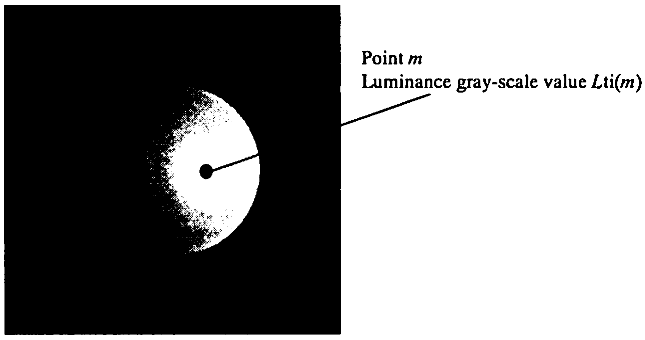

(a)Case of illuminated by the light souce i

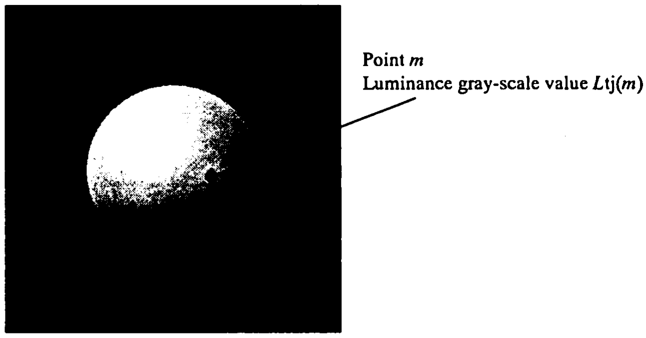

(b)Case of illuminated by the light source j

Fig.10 The gray-level image with highlight.

In this section, a method of estimation of luminance distribution of highlight on gray-level images caused by specular reflection component using an approximate model is introduced. Furthermore, correcting the highlight on gray level image, the result of numerical experiment using the photometric stereo method is described.

Although there are several models applicable to describe the highlight caused by the specular reflection component on object surface, this study focuses only on the model which can be applied to circular highlight on the hemispherical objects. The result of the study is described below.

Two gray-level images with different light source locations are shown in Fig. 10. Fig. 10 (a) is the gray-level image illuminated by light source i and (b) is that of light source j. Then, the highlight is corrected on the gray-level image of Fig (a), and the point m where the luminance gray-scale value is maximum is selected. Here, the vector directed from the point m to the light source is defined as S_{mi}, the normal vector of the object surface at point m as N_m, and the vector from the point m to the viewpoint as V_m. In addition, the luminance gray-scale value at the point m of the image in Fig.10 (a) is defined as $L_{ti}(m)$.

In Fig. 10 (a), $\vec{N}_m$, $\vec{S}_{mi}$ and $\vec{N}_m$ lie on the same plane, and the condition of specular reflection can be shown as follows:

$$\vec{N}_m \bullet \vec{S}_{mi} = \vec{N}_m \bullet \vec{V}_m \quad \cdots\cdots (5)$$

If $\vec{V}_{mi}$, $\vec{S}_{mi}$ and $\vec{N}_m$ are unit vectors, then the angle made by $\vec{N}_m$ and $\vec{V}_{mi}$ and the angle made by $\vec{N}_m$ and $\vec{S}_{mi}$ are equal at point m as indicated in Fig.11, and $\vec{V}_{mi}$ and $\vec{S}_{mi}$ have the same length. Therefore, the normal vector $\vec{N}_m$ can be described as follows:

$$\vec{N}_m = \frac{\vec{S}_{mi} + \vec{V}_m}{k} \quad \cdots\cdots (6)$$
$$\left(\because k = \left|\vec{S}_{mi} + \vec{V}_m\right|\right)$$

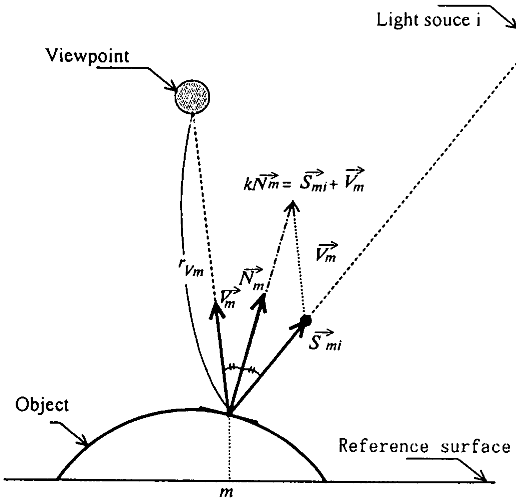

Fig.11 The geometric relation between normal vector at point m, light source and viewpoint.

$L_{ti}(m)$ can be expressed as follows according to the Phong model when the distance between the point m and the light source is rm ,and the luminous intensity of the light source is I:

$$L_{ti}(m) = c \cdot \frac{1}{\pi} \cdot \rho_d \cdot \left(\vec{N}_m \bullet \vec{S}_{mi}\right) \cdot \frac{I}{r_m^{\ 2}} + c \cdot \frac{\left|\vec{N}_m\right|\left|\vec{V}_m\right|}{\left(\vec{N}_m \bullet \vec{V}_m\right)} \cdot \rho_s(\alpha) \cdot \left(\vec{V}_m \bullet \vec{R}_m\right)^n \cdot \frac{I}{r_m^{\ 2}} \quad (7)$$

In expression (7), the coefficient c is a constant, which is dependent on the lens conditions, while $\vec{R}_m$ is a vector directed toward the direction of reflection at the point m. Furthermore, according to the assumption of equation (5), the direction of viewpoint and that of reflection are consistent at point m. Therefore, expression (7) can also be described in the following form.

$$L_{ti}(m) = c \cdot \frac{1}{\pi} \cdot \rho_d \cdot \left(\vec{N}_m \bullet \vec{S}_{mi}\right) \cdot \frac{I}{r_m^{\ 2}} + c \cdot \frac{\left|\vec{N}_m\right|\left|\vec{V}_m\right|}{\left(\vec{N}_m \bullet \vec{V}_m\right)} \cdot \rho_s(\alpha) \cdot \frac{I}{r_m^{\ 2}} \quad (8)$$

The luminance gray-scale value at point m $L_{tj}(m)$ is obtained by the gray-scale image in Fig. 10 (b) by illuminating via the light source j, which has same luminous intensity I and distance rm as light source i, but of different position. If $L_{tj}(m)$ does not include any specular reflection light, then:

$$L_{tj}(m) = c\frac{1}{\pi}\rho_d \cdot \left(\vec{N}_m \bullet \vec{S}_{mj}\right) \cdot \frac{I}{r_m^{\ 2}} \quad \cdots\cdots (9)$$

$\vec{S}_{mi}$ is a vector directed from the point m to the light source j. The following equation is obtained by equation (9) and equation (7):

$$L_{ti}(m) = \frac{\left(\vec{N}_m \bullet \vec{S}_{mi}\right)}{\left(\vec{N}_m \bullet \vec{S}_{mj}\right)} \cdot L_{tj}(m) + c \cdot \frac{\left|\vec{N}_m\right|\left|\vec{V}_m\right|}{\left(\vec{N}_m \bullet \vec{V}_m\right)} \cdot \rho_s(\alpha) \cdot \frac{I}{r_m^{\ 2}} \quad \cdots\cdots (10)$$

Therefore, according to (10), the luminance gray-scale value $L_{tj}(m)$ caused by the specular reflection light at the point m of the gray-scale image in Fig.10 (a) can be calculated by the following equation.

$$L_{ts}(m) = L_{ti}(m) - \frac{\left(\vec{N}_m \bullet \vec{S}_{mi}\right)}{\left(\vec{N}_m \bullet \vec{S}_{mj}\right)} \cdot L_{tj}(m) \quad \cdots\cdots (11)$$

Fig.12 (a) shows a gray-level image of the object surface with the highlight caused by the specular reflection component, while Fig.12 (b) is the luminance gray scale curve on A-A' cross section including the point m, where the luminance gray-scale value is the highest in the highlight. If the luminance gray-scale distribution of the highlight caused by the specular reflection component is assumed to be the luminance gray-scale curve, which is an

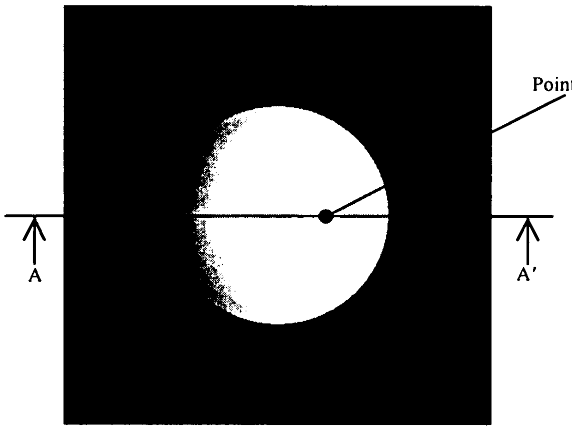

(a)Gray-scale image of the object surface when illuminated by the light source i

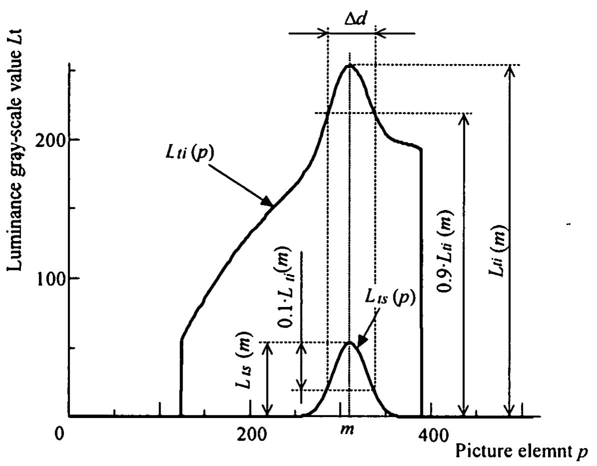

(b)Luminance gray-scale distribution on A-A' cross section.

Fig.12 Gray-level image and luminance gray-scale distribution on A-A' cross section.

approximate model, such as shown in Fig.12 (b), the luminance gray scale curve $L_{ts}(\Delta p)$ can be described as follows:

$$L_{ts}(\Delta p) = C_1 \cdot e^{-C_2 \Delta p^2} \quad \cdots\cdots (12)$$

where Δp is the number of picture elements between a random element and the point *m*, and the coefficient C_1 is the amount of specular reflection light $L_{ts}(m)$ at the above-mentioned point *m*. On the other hand, the coefficient C_2 is determined as follows.

Δd is the number of picture elements between the two points on which the luminance gray scale value is 90 % of the luminance scale value $L_{ti}(m)$ at the point *m*. In equation (12), Δd also indicates the distance between the two points where the luminance scale value is $0.1 \cdot L_{ti}(m)$ less than the maximum value $L_{ts}(m)$. Furthermore, the following equation holds if the two points are located in the position where the number of picture elements, when counting from the point *m*, is equal.

$$L_{ts}(m) - 0.1 \cdot L_{ti}(m) = C_1 \cdot e^{-C_2\left(\frac{\Delta d}{2}\right)^2} \quad \cdots\cdots (13)$$

Therefore, C_2 can be expressed as follows:

$$C_2 = \frac{\ln\left(\frac{L_{ts}(m) - 0.1 \cdot L_{ti}(m)}{C_1}\right)}{\left(\frac{\Delta d}{2}\right)^2} \quad \cdots\cdots (14)$$

As described above, after determining C_1 and C_2 regardless of reflective characteristics of the object surface, the amount of specular reflection light (luminance distribution of the highlight) of each picture element is estimated by equation (12). Then, correction is to be made by subtracting this amount from each picture element of the gray-level image.

When C_1 is 0, it signifies that highlight is not generated on the object surface. When C_1 is less than 0, it should be presumed that highlight has not generated on the object surface, thus correction is not to be made.

4..3 Highlight Correction and Review of Shape Measurement

In this section, the result of the highlight correction implemented to the gray-scale image of the light source i is reviewed. Meanwhile, gray-scale image of light source j is applied to highlight correction for the gray-scale image of light source i.

(a) and (b) of Figure 13 and 14 show the result of comparison of the gray-scale images of the object with a specular reflection component before and after correction, while (c) and (d) compare the isoluminance gray-scale contour of the images before and after correction.

In Fig.13, diffuse reflectance coefficient of the object surface ρd is set to 0.6, specular reflection coefficient ρs (0) to 0.1 and rate of diffusion of light of specular component *n* to 20, while in Fig14, diffuse reflectance ρd is set to 0.4, specular reflectance ρ_s (0) to 0.3 and rate of diffusion of light of specular reflection component *n* to 20.

As indicated in Fig.13, when the ratio of specular reflection component is small, the range from 200 to 250 on the luminance gray scale corresponds to the highlight range. After correction, the luminance gray-scale value in range area has clearly decreased to the level of the luminance gray-scale value of a diffuse reflection component, while the highlight has been eliminated from the gray-scale image. In Fig.14, which has a relatively high specular reflection component ratio, the luminance gray-scale value of the diffuse reflection component become considerably low due to higher luminance of the specular reflection component compared to the above-mentioned case. As a result, the range from 100 to 250 on the luminance gray scale can be said to correspond to the highlight range. After correction, the luminance gray-

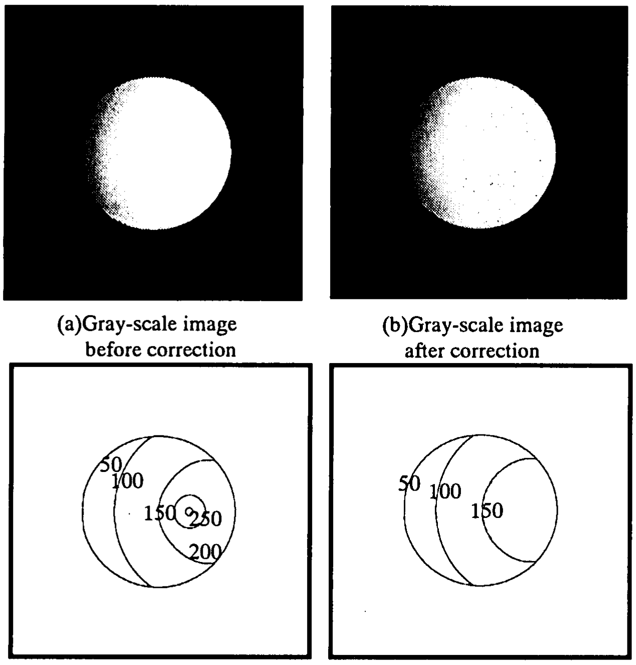

(a)Gray-scale image before correction

(b)Gray-scale image after correction

(c)Isoluminance gray-scale contour before correction

(d)Isoluminance gray-scale contour after correction

Fig.13 The comparison of gray-scale image and isoluminance gray-scale contour before and after correction.

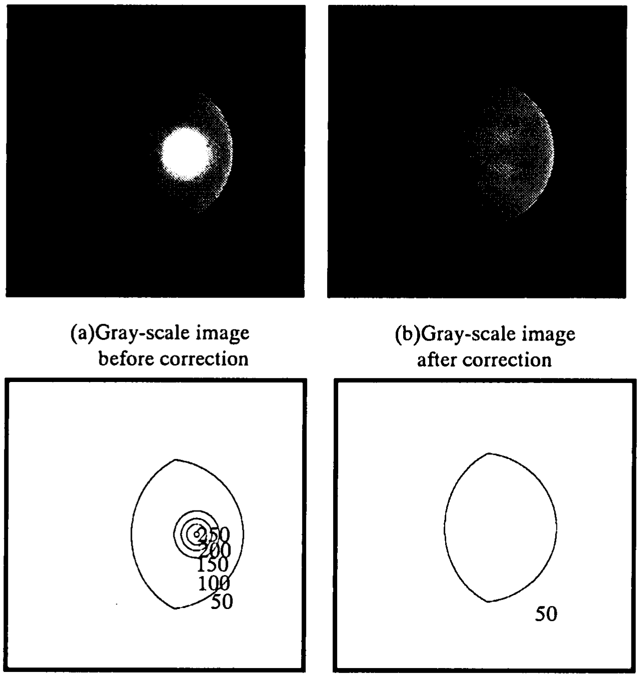

(a)Gray-scale image before correction

(b)Gray-scale image after correction

(c)Isoluminance gray-scale contour before correction

(d)Isoluminance gray-scale contour after correction

Fig.14 The comparison of gray-scale image and isoluminance gray-scale contour before and after correction.

scale value in this range has clearly been lowered to the level of the luminance gray-scale values of the diffuse reflection component, while the highlight has been removed from the gray-scale image. As a result of this, it can be visibly observed that the highlight has been cleared from the gray-scale image after correction.

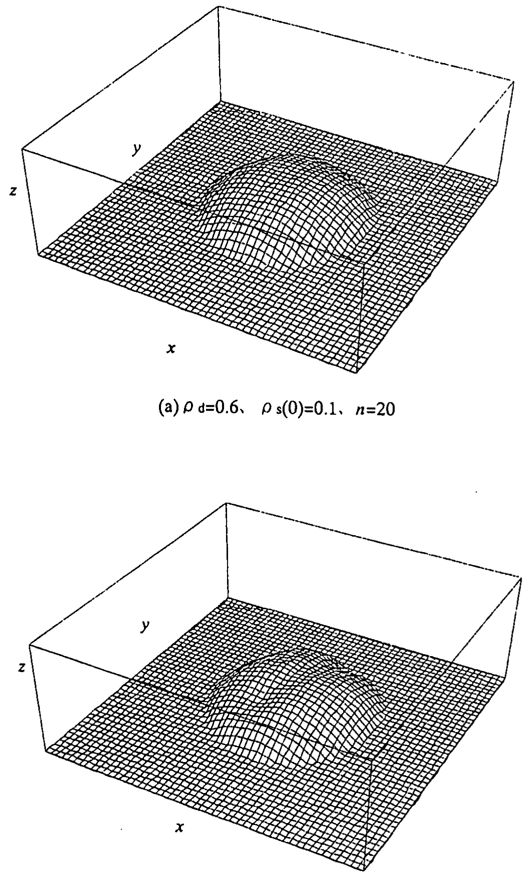

(a) ρ_d=0.6、 $\rho_s(0)$=0.1、 n=20

(b) ρ_d=0.4、 $\rho_s(0)$=0.3、 n=20

Fig15 The comparison of the three-dimensional reconstruction results after correction.

Fig.15 shows the result of three-dimensional reconstruction of the object using the gray-scale images after highlight correction. In Fig.15 (a), the diffuse reflectance coefficient of the object surface ρ_d is set to 0.6, the specular reflection coefficient $\rho_s(0)$ to 0.1 and the rate of diffusion of specular reflection n to 20, while in (b), the diffuse reflectance coefficient ρ_d is set to 0.4, the specular reflectance coefficient $\rho_s(0)$ to 0.3 and the rate of diffusion of specular reflection n to 20. As indicated in Fig.15, when the ratio of the specular reflection component is as small as $\rho_s(0)$ =0.1, the information extracted through the 3-D reconstruction after correction is a good approximation of the actual shape. In case of a higher specular reflection component ratio, which is $\rho_s(0)$ =0.3, the information extracted through the 3-D reconstruction after correction shows a good approximation of the actual shape, except for the occurrence of slight concave part near the zenith.

The reason of the occurrence of concave part near the zenith is that the equation (8) is applied where it no longer holds. This happens because, when the specular reflectance coefficient $\rho_s(0)$ is 0.3 and the rate of diffusion of specular reflection n is 20, highlight is enhanced and the area of highlight becomes wider, thus luminance caused by specular reflection component is included in luminance gray-scale value $L_{is}(m)$ at the point m on the gray-level image illuminated by the light source j.

Fig.16 is a comparison of the two-dimensional cross section of the 3-D reconstruction result of the object before and after correction.

As shown in Fig.16, in case of $\rho_s(0)=0.3$, when the specular reflection component ratio is high, the two-dimensional cross section after correction still has some irregularities near the zenith, although, this has improved.

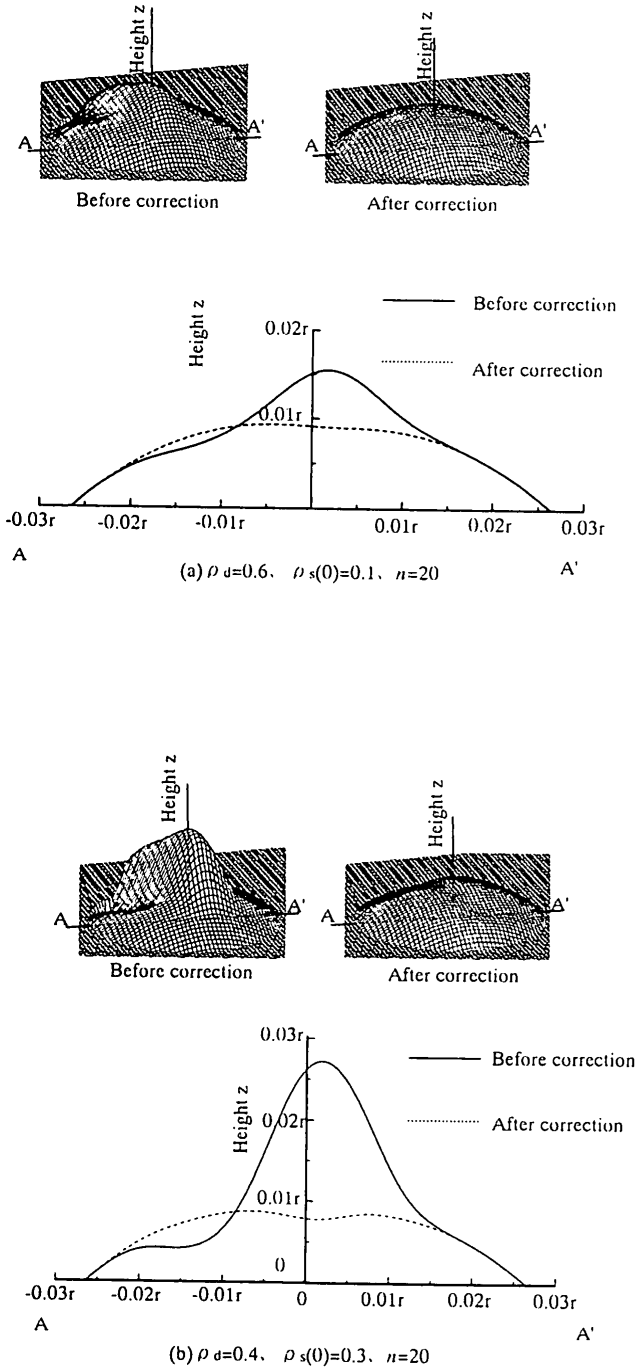

Fig.16 The comparison of the two-dimensional cross section of the reconstruction results.

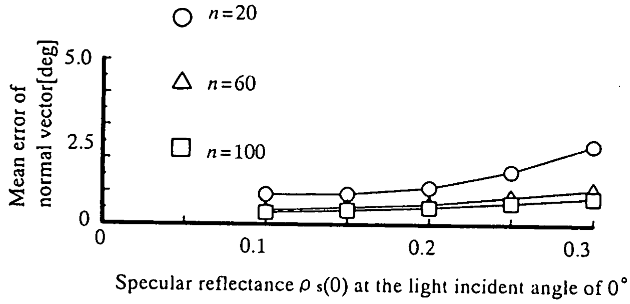

Fig.17 The mean error of normal vector for specular reflectance.

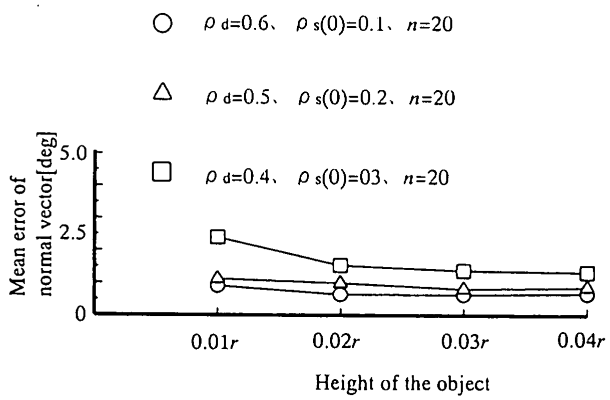

Fig.18 The relationship between the height of the object and the mean error of normal vector.

Fig.17 shows the result of the mean error of the normal vector in its distribution after correction relative to the specular reflectance $\rho_s(0)$ included in the object's total reflectance $\rho = 0.7$. In this figure, the horizontal axis represents the specular reflectance $\rho_s(0)$ included in the total reflectance, while the vertical axis represents the mean error. The symbols plotted on the diagram, ○,△ and □, indicate the rate of diffusion of specular reflection n is 20, 60 and 100, respectively.

As a result, by correcting the highlight, the mean error of the normal vector decreases by approximately 1/5 to 1/10 regardless of coefficient n that represents the rate of diffusion of the specular reflection component

Fig.18 shows the mean error of normal vector in its distribution after correction relative to the height of the hemispherical object with the curvature radius of $0.4r$. The symbols plotted in Fig.18, ○,△ and □, indicate specular reflectance $\rho_s(0)$ as 0.1, 0,2 and 0.3, respectively, which are included in the object's total reflectance ρ of 0.7. When the coefficient n that represents the rate of diffusion of the specular reflection component is set to 20, the mean error of the normal vector rises, as the height lowers. However, the error is within the range of 1[deg] except when $\rho_s(0)=0.3$. Therefore, in cases of the specular reflectance $\rho_s(0)=0.1$ and 0,2, meaningful information concerning the height of the object is obtained.

5. Conclusion

In this study, by first employing the Phong model, the effect of specular reflection component in reflection characteristics of the object surface on shape measurement of the object is reviewed through application of the photometric stereo method.

(1) Case of specular reflectance ρ_s (0) increases, the highlight is enhanced

(2) As the coefficient n, which indicates the rate of diffusion of the light of the specular reflection component becomes smaller, the directivity of specular reflection light becomes lower, and thus the area of highlight is widened.

Therefore, the effect of the specular reflection component increases.

Furthermore, it was clarified that the use of the photometric stereo method in 3-D shape measurement of the object with specular reflection component causes significant error.

In addition, luminance distribution models for the highlight caused by the specular reflection component are introduced in order to eliminate its effect and the method to correct the highlight is reviewed.

As a result, it was found that when the ratio of specular reflection component is small as ρ_s (0) =0.1, the information extracted through both 3-D reconstruction and 2-D cross section shows good approximation of actual object. In case of a higher specular reflection component ratio, such as ρ_s (0) =0.3, the information extracted through 3-D reconstruction and 2-D cross section shows good approximation of actual object, except for the appearance of slight concave part near the zenith. The results obtained suggest that the correction of highlight enables the application of the photometric method to 3-D measurement of hemispherical objects with unknown reflection characteristics, namely those with specular reflection component, just as the method can be applied to objects with a Lambertian surface. Meanwhile, the method proposed in this paper can not be applied to objects with uneven surfaces or those which have specular reflection component strong enough to reflect the light source itself, such as metal objects. Therefore, we plan to continue our study to seek for a measurement method that can be applied to such objects as well.

References

(1)M.F.Wu and H.T.Sheu : Representation of 3D Surfaces by Two-Variable Fourier Descriptor, IEEE Trans. Pattern Analysis and Machine Intelligence, 20-8,pp.858-863(1998).

(2)R.A.Morano, C.Ozturk, R. Conn, S. Dubin, S. Zietz and J.Nissanov : Structured Light Using Pseudorandom Codes, IEEE Trans.Pattern Analysis and Machine Intelligence, 20-3, pp.322-327(1998).

(3)J.A.Noble, R. Gupta, J. Mundy, A. Schmitz and R.I.Hartley : High Precision X-Ray Stereo for Automated 3-D CAD-Based Inspection, IEEE Trans. Robotics and Automation,14-2, pp.292-301(1998).

(4)Megumi Saito , Yoichi Sato, Katsushi Ikeuchi and Hiroshi Kashiwagi : Measurement of surface orientations of transparent objectsusingpolarization in lighlight, J.Inform.Process.Jpn.II, 53-II, 58(1998).

(5)R.J.Woodham : Photometric method for determining surface orientation from multiple images, Optical Engineering, 19-1,No.1,pp.139-144(1980).

(6)H.D.Tagare and R.J.P.deFigueiredo : A Theory of Photometric Stereo for a Class of Diffuse Non-Lambertian, IEEE Trans. Pattern Analysis and Machine Intelligence, 13-2,pp.133-152(1991).

(7)Jun Yang, Noboru Ohnishi and Noboru Sugie : Photometric stereo with two images, J.Inform.Process. Jpn.34-10, pp.2143-2152(1993).

(8)Koichi Shinmoto, Tsunenori Honda and Shunichi Kaneko : Reconstruction of 3D orientationof skin surface replicas by expanding photometric stereo, Trans. Inst. Electron. Inform. Communi. Engnr. Jpn.J77-D-II-9,pp.1797-1805(1994).

(9)Yuuji Iwahori, Noriharu Hiratsuka, Hiroyuki kamei and Shoichiro Yamaguchi : Extended photometric stereo for an object with unknown reflectance property, Trans. Inst. Electron. Inform. Communi. Engnr. Jpn. J71-D-1,pp.110-117(1988).

(10)Ikeuchi : Extracting the Shape and Roughness of Specular Lobe objects Using Four Light Photometric Stereo, IEEE Trans. Pattern Analysis and Machine Intelligence,18-4, pp.449-454(1996).

(11)Kenji Fujinami, Naotaka Ikemoto and Minoru Isomura : On 3-Dimensional measurement of grassy object by photometric stereo.-Fundamental examination on extraction of highligh-, Proc. 1998 Annual Conf. Rec.IEI.Jpn.(in Japanese),pp.260(1998).

(12)Minoru Isomura and Motomi Yamauchi : An approximate calculation of interrefections in rooms with mixed diffuse-specular surface(part2), J. Illum. Engng. Jpn. 67-10,pp.509-513 (1983).